Elsevier Editorial System(tm) for Journal of Catalysis

Manuscript Draft

Manuscript Number:

Title: Pd/TiO2 Doped Faujasite Photocatalysts for Acetophenone Transfer Hydrogenation in a Photocatalytic Membrane Reactor

Article Type: Research paper

Keywords: Photocatalysis, Ketone Hydrogenation, doped Titanium dioxide, Zeolite, Photocatalytic Membrane Reactors, Sustainable Chemistry

Corresponding Author: Professor Raffaele Molinari,

Corresponding Author's Institution: University of Calabria

First Author: Cristina Lavorato

Order of Authors: Cristina Lavorato; Teresa F. Mastropietro; Pietro Argurio; Giuseppe Pirri; Teresa Poerio; Raffaele Molinari

Graphical Abstract (for review)

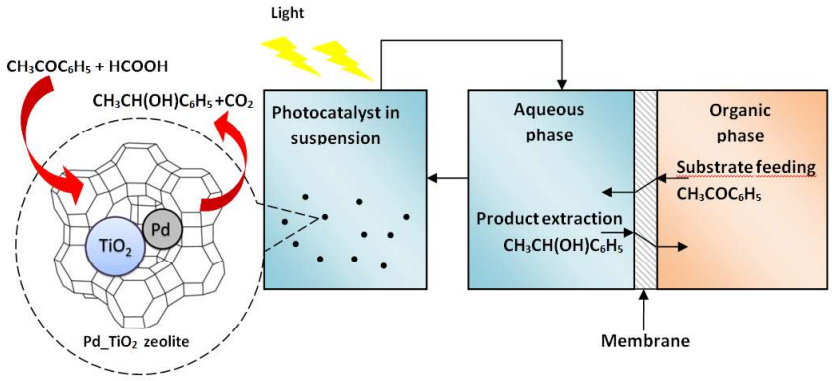

***Highlights (for review)**

- FAU-TiO_2 and Pd-FAU-TiO_2 photocatalysts have been sinthesized and characterized
- Prepared photocatalysts were tested in the transfer hydrogenation of acetophenone
- Tests were conducted in batch and membrane reactor (PMR) under UV and visible light
- Pd addition efficiently extended the UV response of FAU-TiO_2 towards visible light region
- Use of PMR permitted to extract ca. 25% of the product in the organic phase

Pd/TiO_2 Doped Faujasite Photocatalysts for Acetophenone Transfer Hydrogenation in a Photocatalytic Membrane Reactor

Cristina Lavorato [a], Teresa F. Mastropietro[b], Pietro Argurio [a], Giuseppe Pirri [a], Teresa Poerio[b], and Raffaele Molinari [a]*

[a] University of Calabria - Department of Environmental and Chemical Engineering, cubo 44A, Via Pietro BUCCI, 87036 Rende (CS), Italy.

[b] National Research Council - Institute for Membrane Technology (ITM–CNR) c/o University of Calabria, cubo 17C, Via Pietro BUCCI, 87036 Rende (CS), Italy.

(*) Corresponding author. Tel: +39 0984 496699; e-mail: Raffaele.molinari@unical.it

University of Calabria - Department of Environmental and Chemical Engineering, cubo 44A, Via Pietro BUCCI, 87036 Rende (CS), Italy.

Submitted to Journal of Catalysis, June 2017

Abstract

Different FAU-TiO_2 photocatalysts have been prepared and tested in the transfer hydrogenation of acetophenone to phenyl ethanol, an industrially relevant product. Water as solvent, formic acid as hydrogen and electron donor and UV and visible light irradiation, have been employed. The TF10P photocatalyst showed the best homogeneous dispersion of TiO_2 particles on the zeolite surface, BET and pore volume values and photocatalytic performance . A further functionalization of the TF10P catalyst with Pd particles (Pd_TF10P), shifted the catalytic response in the visible range. The productivity obtained by using the Pd_TF10P photocatalyst under visible light was higher than that obtained by using the TF10P under UV light (103.5 mg g_{TiO2}^{-1} $h^{-}1$vs 81.7 mg g_{TiO2}^{-1} h^{-1}). The photocatalytic membrane reactor had an extraction percentage of phenylethanol from the reactive phase to the organic phase of ca. 25%. The overall results evidenced the high potential of this photocatalytic system in the photocatalytic reduction of acetophenone under visible light.

Keywords: Photocatalysis, Ketone Hydrogenation, doped Titanium dioxide, Zeolite, Photocatalytic Membrane Reactors, Sustainable Chemistry.

1. Introduction

In recent years [1], exploitation of photocatalytic reactions in the design of efficient and environment-friendly technologies has attracted great attention. Among the main chemical transformations, currently applied in industrial practices, reduction processes, such as the reduction of carbonyl compounds in the corresponding alcohols, play an important role in organic synthesis [2-4]. In particular, acetophenone (AP) hydrogenation has been widely studied since the resultant reduction product, 1-phenylethyl alcohol or also phenyl ethanol (PE), is a common precursor for the preparation of analgesic and anti-inflammatory drugs as well as fragrances and perfumes [1,5]. Conventional methods for the hydrogenation of AP employ molecular hydrogen and various heterogeneous catalysts [6-9]. On the contrary, only few works have appeared till now on the photocatalytic transfer hydrogenation of AP [10-13], and very few of them use green solvents and hydrogen donors or membrane reactors [1]. To meet the main principles of green chemistry, more sustainable methods to synthesize organic compounds by using mild conditions, cheaper and inherently non-toxic catalysts and, eventually, renewable and greneer resources, such as visible or solar light as irradiation source are needed, in particular, use of water [1] as green solvent for reactions and syntheses could led to the development of cleaner and benign chemical processes. For example, formic acid in aqueous suspensions of TiO_2 was efficient as hole scavenger preventing the

oxidation and the re-oxidation of various nitrobenzenes, also under aerated conditions [14]. Li et al. [15] reported that the photocatalytic hydrogen evolution and decomposition of pollutants using oxalic acid, formic acid or formaldehyde as electron donor can take place simultaneously. Indeed, formic acid is a ‘‘green’’ sacrificial reagent which can be irreversibly converted into carbon dioxide (CO_2) and hydrogen (H_2) [1,15,16].

Semiconductor photocatalysis, especially when activated by visible light, is currently one of the [2, 10, 17-19]. This interest is also motivated by the inexpensiveness and non-toxicity of many semiconductor photocatalysts.

Amoung the various categories of materials that have been studied to be used as semiconductors for different applications, TiO_2 and zeolite-based photocatalysts show a great potential for photocatalytic reactions [17, 20-22].

TiO_2 is currently considered the most promising catalyst for photocatalytic reactions, owing to a suitable band gap energy for redox reactions, high mechanical and chemical stability, environmental friendliness, low cost, and convenience of preparation [23, 24]. Nevertheless, some practical problems include the recombination of photo-generated electron/hole pairs, the poor use of visible ligth, the separation and post-recovery of the suspended catalyst from the reaction batch, and its low adsorption ability for organic molecules at low concentrations.

Combining adsorbents such as zeolites and TiO_2 photocatalysts would help to create advanced photocatalytic systems with improved adsorption. Moreover, zeolites offer high surface area, unique nanoscaled porous structures and ion exchange properties which are profitable for the design of efficient photocatalytic systems [21,22]. The arrangement of cages and channels in crystalline zeolites allows a well-defined spatial arrangement and placement of molecules. Furthermore, zeolites have ion exchange property wich can be utilized for incorporating transition metal ions and can induce specific photo-physical properties, such as control of charge transfer and electron transfer processes [25].

The inability of unmodified TiO_2-based photocatalysts to effectively utilize visible light limits the efficiency of solar-driven photocatalytic reactions. It is therefore desirable to develop photocatalysts which can utilize the visible region of the solar spectrum [1, 11, 18, 19, 26]. Noble metals, including Pt, Au, Pd, Rh, Ni, Cu and Ag have been reported to be very effective for enhancing visible light utilization from TiO_2 photocatalysts. Results of our previous work demonstrated that Pd/TiO_2 photocatalysts can represent an interesting perspective for carrying out chemical transformations of organic substrates under visible light [1].

In this work the incorporation of Pd into a TiO_2 functionalized faujasite framework has been performed with the double aim of extending the catalyst activity in the visible light region and

enhancing the absorbtion properties of the catalyst. While the transition metal improves visible light utilization, the zeolite matrix contributes to delay charges recombination by a mechanism of electron hopping within the framework [25]. In addition, the zeolite acts as support for both TiO_2 and Pd metal particles, which will be homogeneously dispersed in the matrix.

To improve the efficency of the photocatalytic system the reaction was also carried out in a Photocatalytic Membrane Reactors (PMR). PMRs combine the advantages of classical photoreactors (PRs) with those of membrane processes with a synergy of both technologies (*e.g.*: chemical reactions and separation processes are performed in one step), thus minimizing the environmental and economical impact [27]. The membrane allows not only the easy recovery and reuse of the catalyst, immobilized on the membrane or just maintained in suspension, but also the selective separation of the desired product from the reaction mixture, contributing to limit side reactions [1, 2]. On this basis, improvements in terms of yield and selectivity can be expected.

In this work, the photocatalytic properties of TiO_2- loaded faujasite (FAU) zeolite and Pd/TiO_2/FAU have been evaluated in the heterogeneous transfer hydrogenation of AP under UV and visible light in batch tests and in a membrane reactor. Various samples of FAU crystals were prepared by loading different amount of TiO_2 and using bare and suspended FAU crystals. The FAU TiO_2 samples were also loaded with Pd and then they were characterized by TEM, BET and Atomic Absorption Spectroscopy. The activity of sinthesized photocatalysts was screened under visible and UV light in batch tests and then the best samples were tested in the photocatalytic membrane reactor evaluating productivity, produced phenyl ethanol and extracted phenyl ethanol in the organic phase.

2. Experimental

2.1. Materials

Acetophenone Reagent Plus (C_8H_8O, 99% purity), from Sigma Aldrich, was used as substrate and, in the integrated membrane system (reactor-contactor), also as organic extracting phase. NaX zeolite crystals (Sigma-Aldrich) having a mean crystals size of about 2 μm and a Si/Al ratio of 1.5, Titanium isopropoxide ($C_{12}H_{28}O_4Ti$, purity > 97%, density 0.96 mg/mL) from Sigma Aldrich and isopropanol (C_3H_8O, 99.9% purity) from Fluka were used to synthesize TiO_2-Loaded FAU. Titanium dioxide (TiO_2) P25 type from Evonic-Degussa (specific surface area = 44 $m^2\ g^{-1}$, crystallographic phase *ca.* 80% anatase and 20% rutile, band gap 3.2 eV) was used as photocatalyst for reference tests.

Ammonia (NH_3, 30% v/v solution in water), hydrochloric acid (HCl, 37% w/w) from Carlo Erba Reagenti, silver nitrate ($AgNO_3$, purity ≥ 99.0%), Palladium(II) chloride ($PdCl_2$, 99% purity) and sodium borohydride ($NaBH_4$, purity ≥ 99.0%), from Sigma, were used to synthesize home-made Pd/TiO_2-Loaded FAU catalyst.

Formic acid (CH_2O_2, 99% purity) from Sigma Aldrich was used during photocatalytic tests.

Sodium hydroxide pellets (NaOH, 97% purity) from Aldrich was used to adjust the pH of the aqueous solution during the photocatalytic tests.

A hydrophilic microfiltration polypropylene porous membrane (GH-Polypro (GHP), thickness 101 μm; pore size 0.2 μm; typical water flux, 20 mL min^{-1} cm^{-2} at 70 kPa) was used for filtering the aqueous samples to remove the photocatalyst prior to analysis.

An hydrophobic microfiltration polypropylene porous membrane (Accurel, manufactured by Membrana, thickness 142 μm; pore size 0.2 μm; porosity 70%; symmetric structure as indicated by the manufacturer; water contact angle 127° [28]) was used in the membrane contactor.

Ultrapure water was obtained from Milli-Q equipment by Millipore (Billerica, MA, USA).

2.2. Apparatus and Methods

Preliminary experimental tests on the photocatalytic hydrogenation of acetophenone were conducted in the batch photoreactor, schematically reported in Figure 1. It consists of a cylindrical pyrex glass reactor with an immersed lamp. The annular photoreactor, whose volume is 500 mL, is equipped with 3 outputs in its top section for sampling the suspension, blowing argon and degassing. During a photocatalytic reduction the removal of O_2 from the reaction environment, blowing argon before the reaction, was required to improve the reaction rate and selectivity. Indeed, O_2 behaves as a competitive scavenger of the electrons promoted in the conduction band (e_{cb}) of the photocatalyst and is converted to reactive oxygen radical (O_2•). Consequently, after loading the aqueous reacting solution in the photoreactor and prior starting the photocatalytic tests, the system was degassed with argon for 30 minutes and then it was accurately sealed. The photocatalytic tests were carried out by using a medium pressure Hg immersed lamp (125 W, Helios Italquartz) emitting mainly in the UV region, with an emission peak at 366 nm, or a homemade led lamp with the emission spectrum reported in Fig. 2. The lamp was positioned axially inside the reactor. The temperature of the system was maintained at 32°C by means of thermostatically controlled water cinculating in the pyrex glass jacket surrounding the lamp. The solution was magnetically stirred.

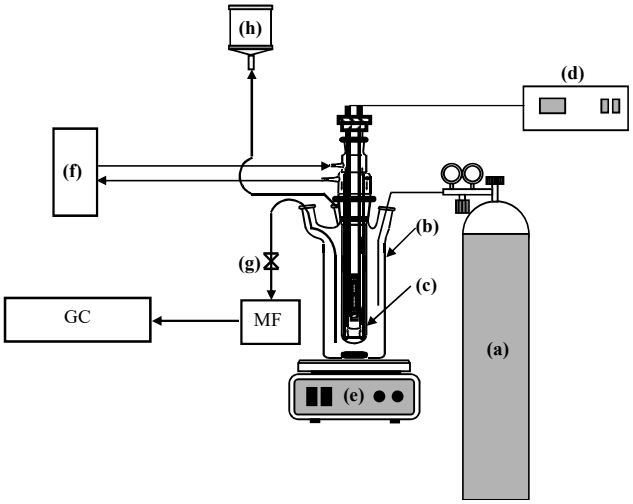

Fig. 1. Scheme of the batch photoreactor: (a) argon cylinder; (b) photoreactor; (c) medium pressure Hg lamp with cooling jacket; (d) power supply; (e) magnetic stirrer; (f) thermostatic bath with cooling water; (g) sampling valve; (h) degassing system; (MF) samples microfiltration; (GC) gas chromatographic analyses.

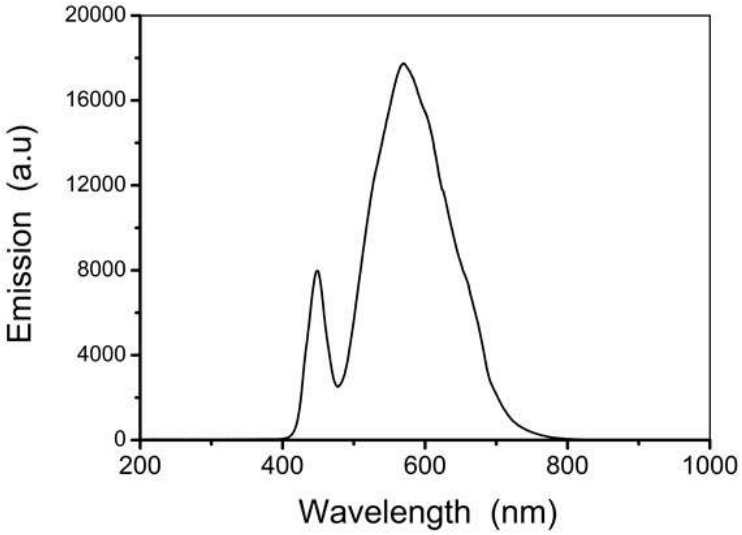

Fig. 2. Emission spectrum of LED immersed lamp.

During the photocatalytic tests, the acqueous solution in the reaction batch was sampled every hour to measure the concentrations of the species involved in the reaction. Each test was carried out for 7 hours. The samples were filtered with a GH-Polypro membrane to remove the catalyst before analysis. All samples were diluted with ethanol 50% before filtering, to avoid adsorption of reactant and products on the polypropylene membrane.

Photocatalytic tests were also performed in the PMR schematized in Figure 3, consisting of a biphasic membrane contactor coupled with the photocatalytic batch photoreactor previously described (see Figure 1). The volume of recirculating solution is 725 mL. The aqueous solution is delivered from the photoreactor to the membrane contactor with a peristaltic pump. Then, the aqueous phase returns in the photoreactor under the action of gravity. The membrane contactor, immersed in a thermostatic bath maintained at the same temperature of the photoreactor, is constituted by two compartment cells (each one with a volume of 125 mL) separated by a flat sheet polypropylene membrane with an exposed membrane surface area of 28.3 cm^2. The first compartment contains the aqueous phase coming from the photoreactor, while the second one contains acetophenone, acting as both the organic extracting phase and the substrate reservoir, mantained under mechanically stirring. The phenylethanol produced in the aqueous phase diffuses through the membrane and then dissolves into the organic extracting phase, where it is preserved from successive over-hydrogenation, with an enhancement of process selectivity. The use of a membrane extractor instead of a traditional liquid/liquid extraction unit avoids the physical mixing between the organic and the aqueous phases, and allows a continuous extraction process. Samples were taken from the organic phases every hour for analyses.

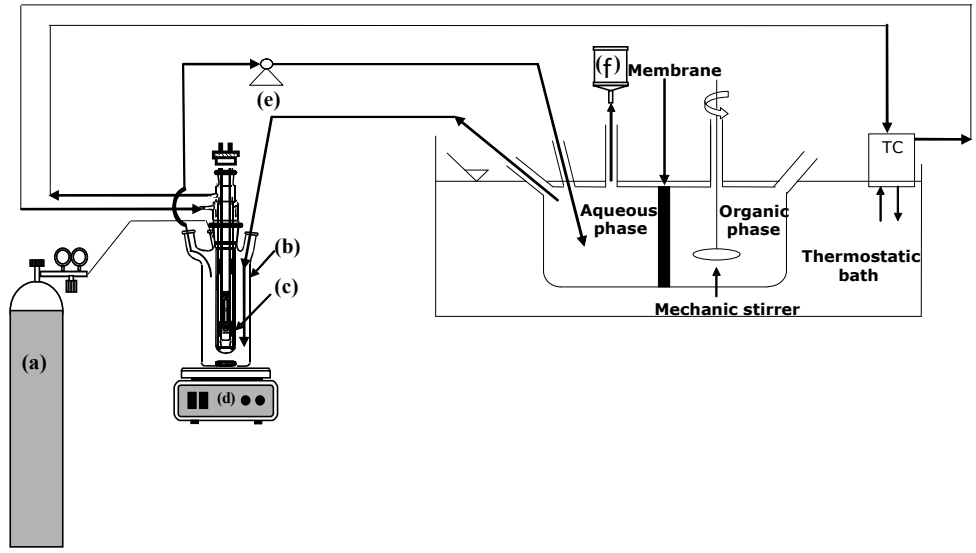

Fig. 3. Scheme of the membrane contactor integrated with the batch photoreactor: (a) argon cylinder; (b) photoreactor; (c) medium pressure Hg lamp with cooling jacket; (d) magnetic stirrer; (e) peristaltic pump; (f) degassing system; (TC) temperature controller.

The photocatalytic tests, both in the batch photoreactor and in the PMR, were carried out using the following operative conditions, optimized in our previous work [1]: acetophenone 0.026M, 1.5 g/L

of photocatalyst, 1.97 M of formic acid as hydrogen and electron donor, pH 7.5, and water as solvent for a total volume of 500 and 725 mL for the batch and the PMR system, respectively. Detection of reaction products was performed by a Gas Chromatograph, Agilent model 6890N equipped with a FID detector and a capillary column SupelcowaxTM 10 (Fused silica, 10 m x 0.1mm x 0.1μm film thickness). After separating the peaks of interest, acetophenone and phenylethanol calibrations were carried out preparing and injecting three times different standard solutions.

A pH meter (WTW Inolab Terminal Level 3) with a glass pH electrode SenTix 81 (WTW) was used for pH measurements.

Obtained results were elaborated using the following parameters:

$$\text{Partition coefficient} = \frac{\text{moles of phenylethanol extracted in the organic phase}}{\text{moles of phenylethanol in the aqueous phase}} \quad (1)$$

$$\text{Extraction percentage} = Q\% = \frac{\text{moles of phenylethanol extracted in the organic phase}}{\text{produced moles of phenylethanol}} \times 100 \quad (2)$$

$$\text{Phenylethanol productivity} = \frac{\text{produced mg of phenylethanol}}{\text{g of catalyst} \times \text{h}} \quad (3)$$

$$TiO_2 \text{ normalized phenylethanol productivity} = \frac{\text{produced mg of phenylethanol}}{\text{g of } TiO_2 \times \text{h}} \quad (4)$$

$$\text{Phenylethanol productivity in the org phase} = \frac{\text{mg of phenylethanol extracted in the org phase}}{\text{g of catalyst} \times \text{h}} \quad (5)$$

2.3. Photocatalysts

2.3.1. Synthesis of TiO_2-Loaded FAU Crystals

- TF10, TF20, TF30

The TiO_2-FAU crystals were prepared from the corresponding Na-FAU zeolite by ion exchange by using 1.85 mL of titanium isopropoxide as precursor (for a theoretical incorporation of ca. 10% w/w TiO_2) which was added drop wise to the zeolite (5 g) under argon flux. This mixture

was carefully stirred for three days and then it was calcined at 500 °C for 1 h. After cooling, the calcined mass was pulverized in an Agate mortar. This composite photocatalyst was indicated as TF10. The preparation of TF20 and TF30 was carried out through a similar procedure using a double and triple amount of titanium isopropoxide, respectively.

- TF10P, TF20P, TF30P

The same amount of titanium isopropoxide before used was added drop wise to the zeolite (5 g) suspended in 30 mL of isopropanol and under argon flux. This mixture was carefully stirred for three days and then it was dried at 60°C (5°C/15 minutes) and calcined at 500 °C for 1 h. After cooling, the calcined mass was pulverized in an Agate mortar. This composite photocatalyst was indicated as TF10P. The preparation of TF20P and TF30P was carried out through a similar procedure using a double and triple amount of titanium isopropoxide, respectively.

2.3.2. Synthesis of Pd/TiO_2-Loaded FAU Crystals

TiO_2-Loaded FAU crystals (4 g) were dispersed in 40 mL of water. The pH was monitored and maintained in the range of 9-10 by adding the opportune amount of ammonia solution (NH_3) to the suspension. The required amount of Pd ($PdCl_2$ acidic solution 0.056 M) for a theoretical incorporation of ca. 1% w/w was added drop wise to the basic TiO_2-Loaded FAU suspension under stirring for 2.5 hours. Then, the mixture was centrifuged at 15000 rpm for 30 minutes by using a Hermle Z383 centrifuge, to recover the modified photocatalyst. The solid was carefully washed with Milli-Q water, to remove excess of chloride ions and ammonia. Small quantities of chloride ions can alter the properties of the catalyst through an activating or poisoning effect. Catalyst washing was repeated till chloride was no more detected in the washing solution, tested with the argentometric method as reported in our previous work [1].

Finally, the resulting catalyst was suspended in 40 mL of Milli-Q water and 18.8 mL of $NaBH_4$ (3.8 mg/mL) was added drop wise to the suspension under stirring at room temperature for 2h. Then the solid sample was dried at 100 °C and pulverized in an Agate mortar. This photocatalyst was indicated as Pd_TF10P.

2.4 Characterization of synthesized catalysts

The morphology, size and distribution of the TiO_2-loaded FAU zeolite samples were investigated by using a Jeol JEM 1400 Plus Transmission Electron Microscope (TEM) at 100 kV in order to get information at a nanoscale level. Surface area, pore volume and pore size distribution of microcrystalline FAU and synthesized catalysts were evaluated by BET (Brunauer–Emmet–Teller) measurements by using a Micromeritics Tristar II analyzer. The samples were analyzed by High-

ResolutionContinuum Source atomic absorption spectrometer (HR-CSAAS) by means of ContrAA700 (Analytik Jena AG, Germany) with a high intensity Xe short arc lamp as continuum source. Samples and standards were fed to the flame by an Injection Module (SFS6), which allowed washing or continuous aspiration of the carrier solution. They were dissolved with hydrofluoric acid and nitric acid followed by dilution in water, subsequently they were acidified with 10% and 1% HCl for Ti and Pd determination, respectively.

Method parameters (i.e. fuel flow and burner height) obtained by the flame automatic optimization procedure for the determination of Ti (N_2O/Acetylene flame) and Pd (Air-acetylene flame) were applied, the absorbance measurements being performed using the spectral lines for Ti at 364.27 nm and for Pd at 244.79 nm.

3.Results and discussion

3.1Photocatalysts characterization

3.1.1 Effect of TiO_2 content and preparation method

Generally the structure of zeolites consists of exchangeable cations such as Ca^{2+}, Na^{+}, K^{+} etc. which are located inside the channels and the cavities of the zeolites framework. From these properties, as reported by Fatimah [29], the preparation of ZnO, ZrO_2 and TiO_2 supported on zeolites can be made by the ion exchange of the precursor cations to make functional material related to the exchanged metals [29]. In our previous research work we synthetized Pd/FAU catalysts by ion exchange of Pd^{2+} from the corresponding Na-FAU zeolite [5]. In this work the preparation of TiO_2/FAU, was conducted by impregnation methods with or without isopropanol as solvent. We hypothesized that the insertion of TiO_2 into porous structure of faujasite occurred by ion exchange of Ti^{4+} cations (from the titanium isopropoxide used as precursor) in faujasite framework and then, by calcination at 500°C, oxide formation of impregnated metal in the anatase crystalline form occurred. As reported by Sun et al. [30] the calcination temperature up to 500 °C is favourable to improve the crystallinity of TiO_2 in the anatase form. On the contrary the TiO_2 sample obtained by using a calcination temperature less than 400 °C is in the amorphous titania form. Instead a calcination temperature from 600 to 700 °C can damage the framework structure of zeolite [30].

The results obtained from the determination by HR-CSAAS of the effective TiO_2 amount in the synthesized TiO_2-FAU crystals are summarized in Table 1. As expected, the percentage of TiO_2 in the samples increased by increasing the amount of titanium isopropoxide used in each synthesis.

The results also indicated that use of isopropanol as solvent assisting the cationic exchange improves a little the amount of TiO_2 loaded in the FAU system.

Table 1. TiO_2 content in TiO_2-FAU crystals

Photo catalysts (TiO_2 -FAU crystals)	**% TiO_2**
TF10	8.0
TF20	14.8
TF30	25.1
TF10P	10.0
TF20P	18.5
TF30P	23.7

TEM images of the samples (Figure 4) show that the formation of aggregates is favoured when the amount of titanium isopropoxide is increased in the synthesis. On the contrary, the presence of the solvent (isopropanol) favours the dispersion of TiO_2 particles, at least when the minor amount of titanium isopropoxide is used during the synthesis. Indeed, in TF10P sample, prepared by using the lowest amount of TiO_2 precursor and isopropanol as solvent, the TiO_2 nanoparticles are quite uniformly distributed on the zeolite surface, guarantying a complete coverage of the crystallites. Conversely, the particle size seems to be less affected by the amount of TiO_2 precursor used in the synthesis or by the presence of isopropanol. TiO_2 particles have a quasi-spherical shape and a quite uniform particle size distribution, with values ranging from ca. 15 to 23 nm. For the other samples, obtained by increasing the amount of titanium isopropoxide during the synthesis, a non homogeneous distribution of titania particles on the zeolite surface can be observed (samples TF20 and TF20P, TF30 and TF30P in Figures 4c-4d and 4e-4f, respectively). The individual particle size is comparable to that reported for TF10P samples, but some agglomerates of greater dimensions (up to 200 nm) stably adhered to the external surface of the zeolite crystals are also visible. In TF30 and TF30P samples, some self-standing agglomerates have been also noticed.

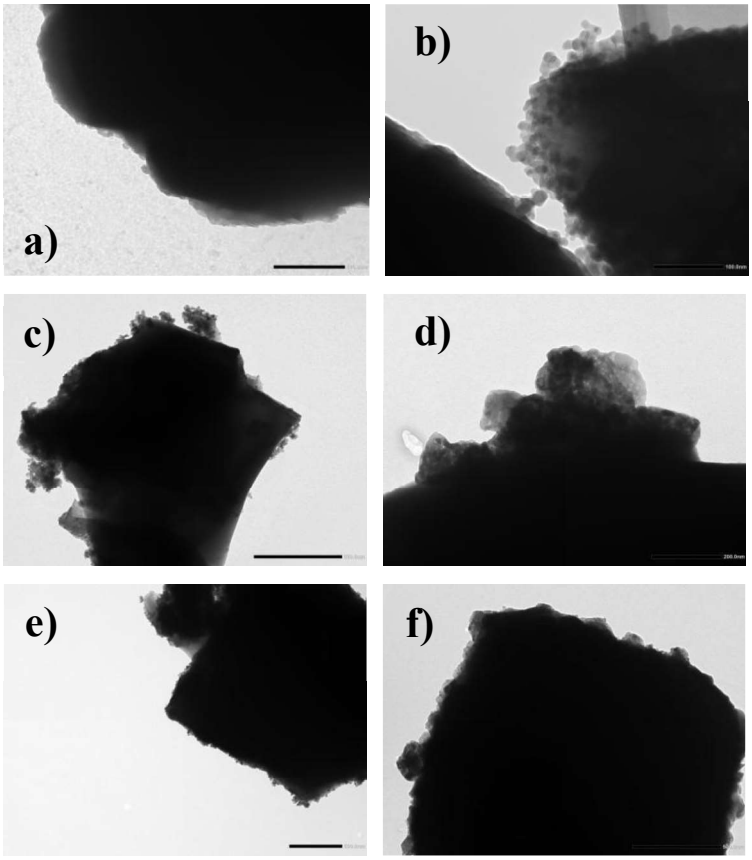

Fig. 4. TEM images of TF10 (a), TF10P (b), TF20 (c), TF20P (d), TF30 (e) and TF30P (f) samples showing the TiO_2 particles distributions on the zeolite surface.

The morphology of the Pd_TF10P sample (Figure 5) obtained by further functionalizing the TF10P sample with Pd nanoparticles, was also characterized by TEM. Pd nanoparticles are quite uniformly distributed within the TiO_2 layer already present on the zeolite surface. The Pd particles, which show a quasi-spherical shape, display a quite uniform particle size distribution, with values ranging from ca. 15 to 27 nm

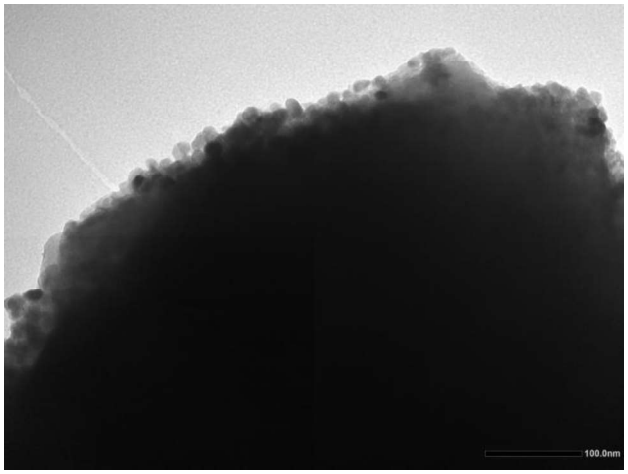

Fig. 5. TEM images of Pd_TF10P samples showing the Pd particles distributions on the zeolite surface.

The textural properties of the microcrystalline TiO_2-FAU and Pd_TiO_2-FAU samples were investigated by determining the pore volume and surface area from nitrogen adsorption isotherms and comparing with the data obtained for pristine FAU microcrystals. Obtained results are reported in Table 2.

Table 2. BET measurements of pristine and TiO_2-loaded FAU-microcrystals.

	Microcristalline FAU	**TF10**	**TF20**	**TF30**	**TF10P**	**TF20P**	**TF30P**	**Pd_TF10P**
BET Surface Area [m^2/g]	616.00	737.23	7.69	586.56	712.04	25.94	564.20	648.74
t-plot External Surface Area [m^2/g]	51.00	41.62	7.51	43.39	41.18	13.93	47.41	41.32
t-plot Micropore Surface Area [m^2/g]	566.00	695.61	0.17	543.17	670.86	12.02	516.78	607.42
t-plot Micropore Volume [cm^3/g]	0.23	0.28	0.00	0.22	0.28	0.01	0.21	0.23
Adsorption average pore width(4V/A by BET) [nm]	1.70	1.67	7.57	1.85	1.76	6.90	1.83	1.57
BJH Adsorption average pore diameter (4V/A) [nm]		3.30	9.66	6.05	7.67	11.59	4.63	4.37
BJH Desorption average pore diameter (4V/A) [nm]		4.52	9.82	6.81	5.95	12.54	5.43	4.20

As it can be seen, TF20 and TF20P show a very low BET surface area and micropore volume if compared with the other samples and with the pristine FAU, which can be attributed to the formation of TiO_2 nanoparticles within the micropores of the zeolite, as well as on the external surface. Melicchio et al. [31] reported that an excess of deposition of TiO_2 on zeolites (SBA-15) cause the formation of large TiO_2 particles reducing the lumen of the mesopores. Surprisingly at

higher amount of TiO_2 precursor, the BET surface area and micropore volume decrease slightly with respect to the pristine FAU sample. We can hypothesize that, by increasing the amount of titania precursor the dimension of particle aggregates increases too. Consequently, these particles can hardly enter into the porous structure of the faujasite zeolite and are mostly deposited on the external surface, partially blocking the pore entrance.

3.2. Photocatalytic hydrogenation of acetophenone in the batch photoreactor

Some photocatalytic tests were performed in the batch photoreactor to study the photocatalytic performance of the homemade TiO_2 loaded FAU and Pd_TiO_2 loaded FAU in the heterogeneous photocatalytic transfer hydrogenation of AP under UV and visible light.

The possible photoreaction mechanism of this multi-component system was reported by Dubey et al. [25]. As they explained, zeolites are amphoteric and they may be used as both electron donors and acceptors owing to the presence of Lewis acid and basic sites. In this case, the irradiation of TiO_2 results in the formation of electron-rich centers and holes. The zeolite is able to donate electrons to the TiO_2 holes, which are consequently transferred to the zeolite framework, thus facilitating charges separation. Similarly, the electrons of the conduction band (CB) of TiO_2 can be transferred to the zeolite electron acceptor sites, that is coordinated aluminium in the framework, and subsequently to the Pd metal particles in the pores, further delaying charge recombination.

As already underlined, the tranfer hydrogenation is carried out by using water as solvent and formic acid as both electron and hydrogen donor. The equation of the reaction is the following:

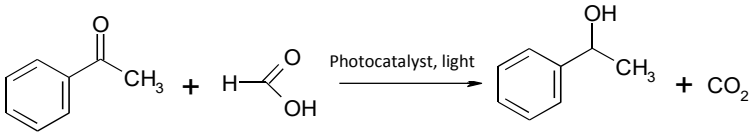

(8)

It can be seen that, stoichiometrically, the moles of the consumed reagent are equal to the moles of formed phenylethanol. However, both the acetophenone and the phenylethanol can generate by-products, thus lowering the yield of the reaction.

3.2.1. Screening of the sinthesized photocatalysts: UV photocatalytic activity.

Preliminary tests were performed in a batch photoreactor to study the photocatalytic activity of the home-made TiO_2 loaded FAU photocatalysts: TF10, TF20, TF30, TF10P, TF20P, and TF30P.

The aim of this screening was to determine the influence of how the different preparative methods and the resulting morphological features of the synthesized catalyst on the final properties and the

photocatalytic performance. From the photocatalytic results, the best catalyst was selected and then it was further modified with Pd noble metal to improve both visible light absorption and activity. The photocatalytic tests with the six samples were conducted in the same experimental conditions, reported in paragraph 2.2, and compared with commercial TiO_2 as control.

As showed in Figure 6, the highest productivity values have been observed for TF10 and TF10P, that are the samples containing the lowest amount of TiO_2 wich is distributed in the form of well-shaped and well-dispersed nanoparticles as seen in paragraph 3.1.1. On the contrary, the productivity values decrease by using the samples containing higher amount of TiO_2 deposited on/or within the FAU crystals. This behaviour can be explained by taking into account the morphology of the TiO_2 particles deposited on the zeolite surface, indeed they are mainly located deep into the zeolite pores (TF20 and TF20P) or mainly present as agglomerates (TF30 and TF30P). As reported by several authors, the photocatalytic activity is highly influenced by the particle size and their distribution on the support surface [17].

As already observed, best results in terms of productivity were obtained by using TF10P as photocatalyst. This one was prepared by using the lowest amount of titanium isopropoxide as TiO_2 precursor and isopropanol as solvent. The presence of the solvent facilited the ionic exchange and permitted to obtain a better dispersion of TiO_2 particles with respect to the other TiO_2-FAU samples. The lower TiO_2 content favourably allowed to maintain a high surface area for the zeolite and a good dispersion of TiO_2 particles on the surface, finally improving the photocatalytic performance of the system.

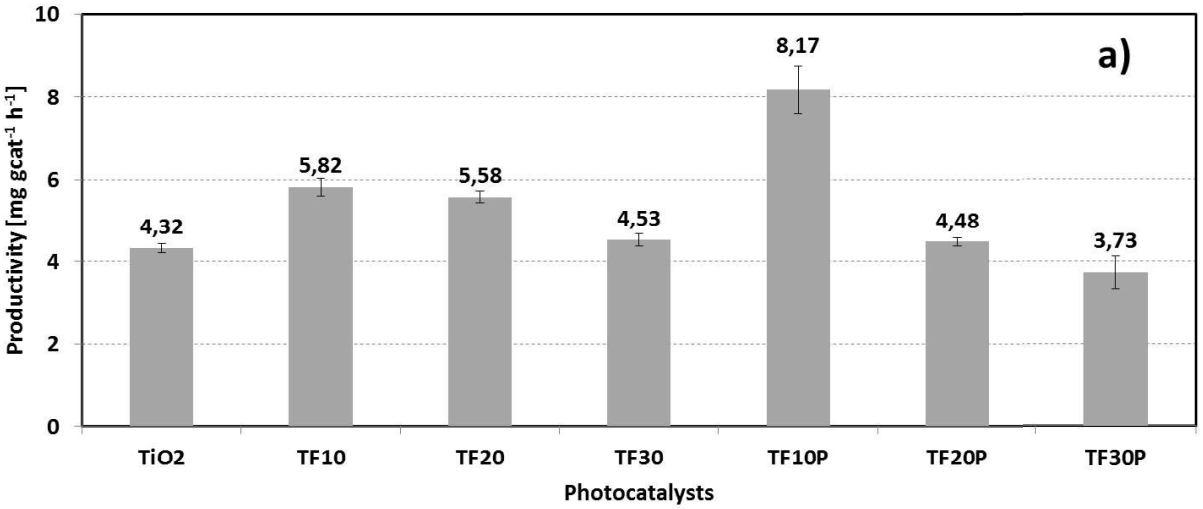

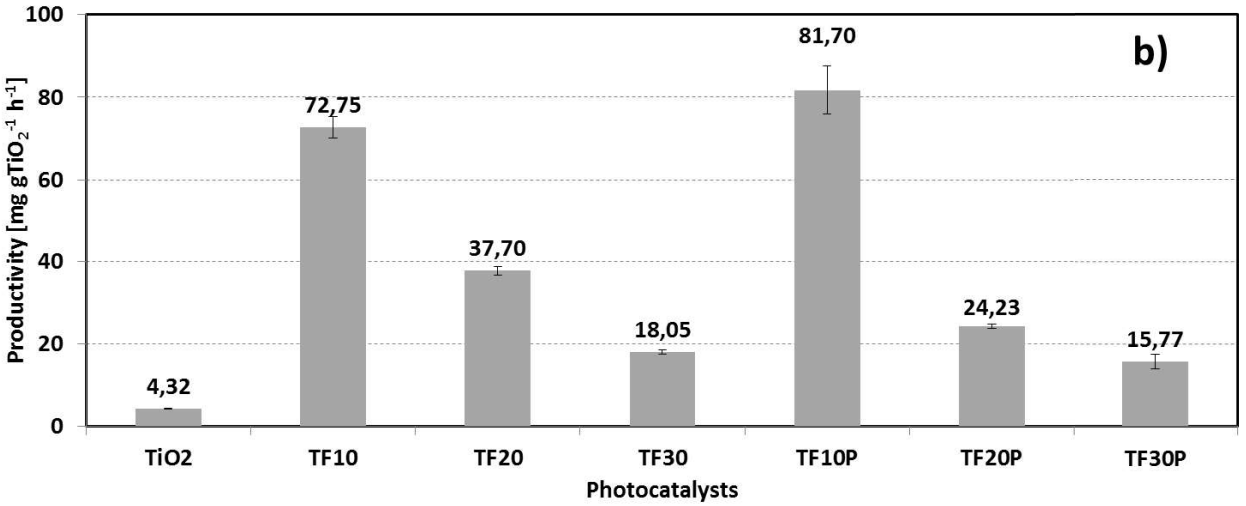

Fig. 6. Comparison of (a) productivity (b) TiO_2 normalized productivity obtained by using commercial FAU, TF10, TF20, TF30, TF10P, TF20P and TF30P as photocatalysts in the batch photoreactor under UV light (operating conditions [HCOOH] = 2 M, TiO_2 1.5 g L^{-1}, pH 7.5, T = 32 °C, test duration = 7 h).

Since the home-made TiO_2-FAU crystals differ in TiO_2 content (see Table 1), the productivity value normalized with respect to TiO_2, was also calculated. The results, reported in Figure 6, further confirm that best performances are obtained by using TF10P as photocatalyst, with a normalized productivity equal to 81.7 ± 5.8 mg g_{TiO2}^{-1} h^{-1}.

3.2.2. Screening of photocatalysts: visible light photocatalytic activity

To determine the visible light activity of TF10P sample, this photocatalyst, the commercial TiO_2 and FAU as control were tested in the batch photoreactor by using the led immersed lamp, emitting in the visible spectrum with λ >400 nm (see Figure 2), as the radiation source, the results are reported in table 3. As expected, the commercial TiO_2 and FAU crystals were inactive under visible light. The same result was obtained also for the TF10P photocatalyst, which did not show any photocatalytic activity by using the visible radiation.

To induce the visible light absorption, the TiO_2 loaded FAU framework was further functionalized with Pd particles.

The Pd_TF10P photocatalyst was sinthesized by deposition/precipitation of palladium nanoparticles on TF10P particles as described in paragraph 2.3.2. The results obtained by testing it in the batch reactor showed that the Pd_TF10P photocatalyst was able to use the visible light for the

photocatalytic transfer hydrogenation of acetophenone, with a productivity value of 10.35 ± 1.21 mg g_{cat}^{-1} h^{-1} (see table 3).

Table 3. Productivity and produced phenylethanol obtained by using commercial FAU, commercial TiO_2, TF10P and Pd_TF10P as photocatalysts in the batch photoreactor with visible light radiation. (Operating conditions: [HCOOH] = 2 M, catalyst 1.5 g L^{-1}, pH 7.5, T = 32 °C, test duration = 7 h).

Photocatalyst	Productivity [mg g_{cat}^{-1} h^{-1}]	Productivity [mg g_{TiO2}^{-1} h^{-1}]	Produced phenylethanol (μmol)
TiO_2	n.d.	n.d.	n.d.
FAU	n.d.	n.d.	n.d.
TF10P	n.d.	n.d.	n.d.
Pd_TF10P	10.35 ± 1.21	103.50 ± 12.10	445 ± 52

n.d.= not detectable

Furthermore, as reported in table 4, the productivity value obtained by using the Pd_TF10P photocatalyst under visible light, was higher than that obtained by using the TF10P under UV light. These results are interesting in the perspective of exploiting sunlight radiation in the chemical synthesis.

Table 4. Productivity and produced phenylethanol obtained during the test into the batch photoreactor by using TF10P and Pd_TF10P photocatalysts under UV and visible light. (Operating conditions: [HCOOH] = 2 M, catalyst= 1.5 g L^{-1}, pH 7.5, T = 32 °C, test duration = 7 h).

Photocatalyst	Radiation	Productivity [mg g_{cat}^{-1} h^{-1}]	Productivity [mg g_{TiO2}^{-1} h^{-1}]	Produced phenylethanol (μmol)
TF10P	UV	8.17 ± 0.58	81.70 ± 5.80	351 ± 25
Pd_TF10P	>400 nm	10.35 ± 1.21	103.5 ± 12.1	445 ± 52

It must be noticed that collected date permit to compare the photocatalytic process vs. the catalytic process in the same reaction which is the transfer hydrogenation of acetophenone. In our previous work [5] we synthetized Pd-loaded FAU crystal and tested it as catalyst in this reaction in a batch reactor using sodium formate as hydrogen donor and water as solvent at a temperature of 60°C for 24 h. An higher productivity value has been obtained by using the photocatalytic approach compared to the catalytic one. The productivity obtained after 7 h of irradiation by using the Pd_TF10P photocatalyst under visible light was higher than that obtained by using the Pd-loaded FAU crystal catalyst after 24 h of reaction (productivity 10 mg g_{cat}^{-1} h^{-1} vs 2 mg g_{cat}^{-1} h^{-1} and 1035 mg g_{Pd}^{-1} h^{-1} vs 144.6 mg g_{Pd}^{-1} h^{-1}).

3.3. Photocatalytic activity in the Photocatalytic Membrane Reactor

To improve the efficency of the photocatalytic system, the behaviour of the Pd-TiO_2 loaded FAU sample was tested under visible light in the PMR described in section 2.2. In this system the photocatalytic reaction and the separation process take place simultaneously. Acetophenone contained in membrane contactor acted as both reagent and extracting phase.

Photocatalytic tests were carried by using the following operating conditions: 1.5 g L^{-1} of Pd_TF10P, 2 M of formic acid as hydrogen and electron donor, adding NaOH addition to rise to pH 7.5, and water as solvent for a total volume of 725 mL.

As described in section 2.2, the total volume and the irradiated volume in which the photocatalyst is dispersed differ in batch and PMR configurations. As reported by some authors, the ratio between the irradiated volume and the total volume (Vi/Vt) can influence system performance [27, 32]. Molinari et al. [27] proposed various reactor configurations for coupling photocatalysis and membrane processes in water purification. They reported that degradation of 4-nitrophenol (4-NP), was enhanced by increasing the percentage of irradiated volume.

In the present work, the photocatalyst suspension (500 mL) is totally irradiated in the batch photoreactor, while in the PMR (725 mL) only ca. 70% (that is 500 mL) of the total aqueous suspension was irradiated during test. Furthermore, during these tests, a deposition of ca. 10% Pd_TF10P particles in the tubes was observed. For this reason, to compare batch and PMR systems, the productivity value was calculated with respect to the amount of photocatalyst effectively irradiated.

System performance was evaluated in terms of amount of produced phenylethanol (μmoles), extraction percentage (Q%), phenylethanol productivity in relation to the gram of photocatalyst effectively irradiated photocatalyst and phenylethanol productivity in the organic phase.

The results, compared with those obtained in the batch system, are summarized in Table 5.

Table 5. Produced and extracted phenylethanol, phenylethanol productivity and extraction percentage (Q %) by using the PMR and the batch photoreactor. (Operating conditions: [HCOOH] = 2 M, Pd_TF10P 1.5 g L^{-1}, pH 7.5, recirculating flow rate = 166 mL min^{-1}, T = 32 °C, test duration = 7 hours).

System	Productivity [mg $g_{cat\ irradiated}^{-1}$ h^{-1}]	Productivity [mg $g_{TiO2\ irradiated}^{-1}$ h^{-1}]	Produced phenylethanol (μmol)	Extracted phenylethanol (μmol)	Q (%)
PMR	9.96 ± 0.89	99.6 ± 8.9	385 ± 34	87.0 ± 0.8	22.8 ± 2.2

Batch	10.3 ± 1.2	103.5 ± 12.1	445 ± 52	NA	NA

*NA = not applicable

Results show that phenylethanol productivity obtained in the PMR and in the batch photoreactor are comparable. The main advantage of using the PMR is the simultaneous removal of the product, which is thus preserved from subsequent reduction. The effectiveness of coupling can be also seen by the value of the partition coefficient after 7 h. It was 1.75 by considering that concentration of phenyl ethanol was 0.7 mmol/L in the organic phase and 0.4 mol/L in the aqueous phase. The extraction percentage of phenylethanol from the reactive phase in the organic phase Q% was 22.8 ± 2.2%, indicating that 25% of produced phenylethanol was extracted into the organic phase. During the photocatalytic tests in the PMR system, the concentration of phenylethanol in the organic phase increased quite linearly (Fig. 7). It can be seen that at 7 h (duration of the test) there is still a positive slope. This means that increasing the time of a reaction an higher value of Q% can be obtained.

In our previous work [1] we synthetized Pd-TiO_2 and tested it as catalyst in this reaction in a PMR reactor under the same operative conditions. In the present work an higher productivity value for gram of TiO_2 has been obtained using the Pd_TF10P compared to Pd_TiO_2 (productivity 99.6 mg g_{TiO2}^{-1} h^{-1} vs 22 mg g_{TiO2}^{-1} h^{-1}).

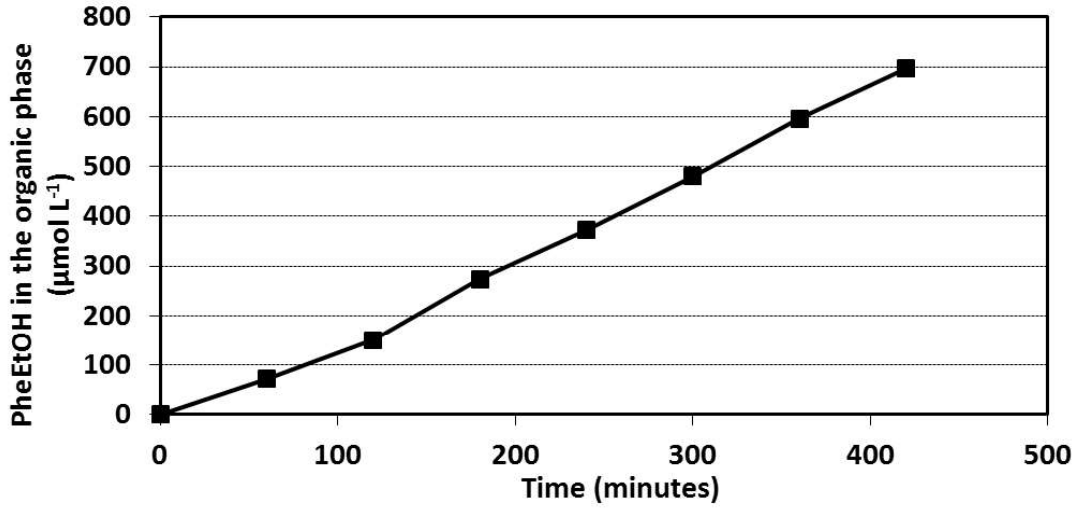

Fig. 7. Phenylethanol concentration in the organic phase vs. time by using the membrane photoreactor with Pd_TF10P photocatalyst. (Operating conditions [HCOOH] = 2 M, catalyst= 1.5 g L^{-1}, pH 7.5, T = 32 °C, test duration = 7 h).

4. Conclusion

Different multi-component catalysts were prepared by functionalizing FAU zeolite sieves with TiO_2 and Pd nanoparticles and tested in the photocatalytic transfer hydrogenation of acethophenone activated by UV and visible radiation. While TiO_2 acts as active photocatalyst, the role of the zeolite matrix is: i) support and scaffold for the TiO_2 particles; ii) active material hampering the recombination of photogenerated charges; iii) support of Pd clusters or nanoparticles; iv) absorbent for the substrate molecules.

The final properties of the catalyst are strictly related both to the initial amount of TiO_2 precursor used in the synthetic procedure and the presence of solvent during the ion exchange process. A highly homogeneous dispersion of TiO_2 catalyst particles on the zeolite surface was obtained in TF10P, prepared by using the lowest amount of TiO_2 precursor and isopropanol as solvent. The highest BET and porous volume values were also obtained for this sample. Accordingly, the TF10P sample showed the best performance in the bacth photoreactor under UV light. The reaction was performed by using water as solvent and formic acid as hydrogen donor, with the aim of designing a green and sustainable process. The TF10P catalyst was further functionalized with Pd particles (Pd_TF10P) in order to shift the photocatalytic response in the visible range. Tests performed both in a bacth reactor and in a PMR showed the high potential of this last catalytic system in the photocatalytic reduction of acetophenone driven by visible light. It is notheworthy that the synergic coupling of TiO_2 and FAU allowed to obtain an homogenous and stable dispersion of the photocatalyst on the support FAU particles, a more effective utilization of light and the efficient charge-transfer to the substrate molecules. The productivity obtained in the membrane reactor was higher in this work compared to a previous our work (productivity 99.6 mg g_{TiO2}^{-1} h^{-1} vs 22 mg g_{TiO2}^{-1} h^{-1}). In particular, the membrane supply gradually a low soluble reactant (acetophenone in the present work) in the reaction ambient and permits to extract simultaneously the product from the reaction ambient. Results are interesting in the perspective of exploiting sunlight radiation in the chemical synthesis and in using photocatalytic membrane reactors.

Acknowledgments: Research partially funded by the European Union Seventh Framework Programme (FP7/2007-2013) under DEMCAMER project (NMP3-LA-2011-262840).

4. References:

[1] R., Molinari, C. Lavorato, P. Argurio, Chem. Eng. J. 274 (2015) 307, doi:10.1016/j.cej.2015.03.120.

[2] R., Molinari, P. Argurio, C. Lavorato, Current Organic Chemistry, 21 (2013) 2516, doi: 10.2174/13852728113179990063.

[3] T. Pasini , A. Lolli , S. Albonetti , F. Cavani , M. Mella, Journal of Catalysis 317 (2014) 206, doi.org/10.1016/j.jcat.2014.06.023.

[4] F. Alonso, P. Riente, F. Rodríguez-Reinoso, J. Ruiz-Martínez, A. Sepúlveda-Escribano, M. Yus, Journal of Catalysis 260 (2008) 113, doi.org/10.1016/j.jcat.2008.09.009.

[5] R., Molinari, C. Lavorato, T.F. Mastropietro, P. Argurio, E. Drioli, T. Poerio, Molecules 21 (2016) 394, doi:10.3390/molecules21030394.

[6] F. Gao, A.D. Allian, H. Zhang, S. Cheng, M. Garland, J. Catal. 241 (2006) 189.

[7] M. Lenarda, M. Casagrande, E. Moretti, L. Storaro, R. Frattini, S. Polizzi, Catal. Lett. 114 (2007) 79, doi: 10.1007/s10562-007-9046-4.

[8] Y. Wang, N. Su, L. Ye, Y. Ren, X. Chen, Y. Du, Z. Li, B. Yue, S.C.E. Tsang, J. Catal., 313 (2014) 113, doi: 10.1016/j.jcat.2014.03.004.

[9] N.M. Bertero, C.R. Apesteguia, A.J. Marchi, Appl. Catal. A Gen. 349 (2008) 100, doi: 10.1016/j.apcata.2008.07.014

[10] S. Kohtani, M. Mori, E.Yoshioka, H. Miyabe, Catalysts, 5 (2015) 1417, doi:10.3390/catal5031417

[11] S. Kohtani, S. Nishioka, E. Yoshioka, H. Miyabe, Catalysis Communications 43 (2014) 61, doi: 10.1016/j.catcom.2013.09.006

[12] S. Kohtani, E. Yoshioka, K. Saito, Kudo A., Miyabe H., Catalysis Communications 11 (2010) 1049, doi: 10.1016/j.catcom.2010.04.022

[13] L. Xiaobin, D. Sun, R. Yuan, X. Fu, Z. Li, Journal of Catalysis 304 (2013) 1, doi: 10.1016/j.jcat.2013.04.004

[14] K. Imamura, S. Iwasaki, T. Maeda, K. Hashimoto, B. Ohtani, H. Kominami, Phys. Chem. Chem. Phys. 13 (2011) 5114, doi: 10.1039/c0cp02279a

[15] Y. Li, G. Lu, S. Li, , Chemosphere 52 (2003) 843, doi: 10.1016/S0045-6535(03)00297-2

[16] N. Wehbe, M. Jaafar, C. Guillard, J.-M. Herrmann, S. Miachon, E. Puzenat, N. Guilhaume, Appl. Catal. A Gen. 368 (2009) 1, doi.org/10.1016/j.apcata.2009.07.038

[17] P. Dutta, Y. Kim Opinion in Solid State and Materials Science 7 (2003) 483, doi: 10.1016/j.cossms.2004.02.004

[18] C. Lavorato, A. Primo, R. Molinari, and H. García. Chem. Eur. J., 2014, 20, 187 – 194. doi: 10.1002/chem.201303689

[19] M. Latorre-Sánchez, C. Lavorato, M. Puche, V. Fornés, R. Molinari, H. Garcia, Chem. Eur. J. 18 (2012) 16774, DOI: 10.1002/chem.201202372

[20] M. Huang, C. Xu, Z. Wu, Y. Huang, J. Lin, J. Wu, Dyes and Pigments 77 (2008) 327, doi: 10.1016/j.dyepig.2007.01.026

[21] Y. Kuwahara, J. Aoyama, K. Miyakubo, T. Eguchi, T. Kamegawa, K. Mori, H. Yamashita, Journal of Catalysis 285 (2012) 223, doi: 10.1016/j.jcat.2011.09.031

[22] A. Corma and H. Garcia. Chem. Commun. (2004) 1443, doi: 10.1039/B400147H

[23] A. Fujishima, K. Honda, Nature 238 (1972) 37, doi:10.1038/238037a0

[24] A. Fujishima, T.N. Rao, D.A. Tryk, J. Photochem. Photobiol. C 1 (2000) 1. doi: 10.1016/S1389-5567(00)00002-2

[25] N. Dubey, S. S.Rayalu, N. K. Labhsetwar, R. R. Naidu, R.V. Chatti, S. Devotta, Applied Catalysis A: General 303 (2006) 152, doi: 10.1016/j.apcata.2006.01.043

[26] J. Lim, P. Murugan , N. Lakshminarasimhan, J. Y. Kim, J. S. Lee, S.-H. Lee , W. Choi, Journal of Catalysis 310 (2014) 91, doi: 10.1016/j.jcat.2013.05.014

[27] R. Molinari, L. Palmisano, E. Drioli, M. Schiavello Journal of Membrane Science 206 (2002) 399–415. doi.org/10.1016/S0376-7388(01)00785-2

[28] R. Molinari, P. Argurio, T. Poerio, Appl. Catal. A Gen. 437(2012) 131, doi.org/10.1016/j.apcata.2012.06.027

[29] I. Fatimah,. Sustainable Energy and Advanced Materials. 1717 (2016) doi: 10.1063/1.4943429.

[30] Q. Sun, X. Hu, S. Zheng, Z. Sun, S. Liu, H. Li Powder Technology 274 (2015) 88, doi: 10.1016/j.powtec.2014.12.052

[31] Melicchio A., Liguori P. F., Russo B. Golemme G., International Journal of Hydrogen Energy, 41 (2016) 5733, doi.org/10.1016/j.ijhydene.2016.02.050

[32] Fischer, M. Kuhnert, R. Glaser, A. Schulze, RSC Adv. 5 (2015) 16340, 10.1039/C4RA16219F

***Research Highlights**

- FAU-TiO_2 and Pd-FAU-TiO_2 photocatalysts have been sinthesized and characterized
- Prepared photocatalysts were tested in the transfer hydrogenation of acetophenone
- Tests were conducted in batch and membrane reactor (PMR) under UV and visible light
- Pd addition efficiently extended the UV response of FAU-TiO_2 towards visible light region
- Use of PMR permitted to extract ca. 25% of the product in the organic phase